In-situ transmission electron microscopy investigation of the influence of hydrogen on the oxidation mechanisms of fine grained magnesium

Xavier Sauvage, Simona Moldovan, Fabien Cuvilly, M. Bahri, T. Grosdidier

In-situ Transmission Electron Microscopy investigation of the influence of hydrogen on the oxidation mechanisms of fine grained magnesium

X. Sauvage[1], S. Moldovan[1], F. Cuvilly[1], M. Bahri[2], T. Grosdidier[3]*

1- Normandie Univ, UNIROUEN, INSA Rouen, CNRS, Groupe de Physique des Matériaux, 76000 Rouen, France

2-Institut de Physique et Chimie des Matériaux de Strasbourg (IPCMS), Strasbourg University, CNRS, 67000 Strasbourg, France

3- Université de Lorraine, Laboratoire d'Etude des Microstructures et de Mécanique des Matériaux (LEM3 UMR 7239), 7 Rue Felix Savart, Metz F-57073, France

*Corresponding author: xavier.sauvage@univ-rouen.fr

Keywords

Magnesium; hydrogen; in-situ microscopy; grain boundaries; oxidation

Abstract

Magnesium oxide is of critical importance for the properties of magnesium alloys designed for solid state storage of hydrogen. The oxidation of Mg was investigated by in-situ transmission electron microscopy under vacuum conditions and 10^5 Pa of H_2 with a special emphasis on the influence of grain boundaries. In agreement with thermodynamic predictions, nucleation and growth of MgO was observed in both conditions, but the mechanisms and the corresponding kinetic are very different. Under vacuum it is assisted by Mg sublimation and relatively fast, while under H_2 the oxidation proceeds slowly along grain boundaries that act as nucleation sites.

1. Introduction

Hydrogen storage in solid state materials has attracted a wide interest during the past years since it is considered as one of the safest and most effective for mobile applications [1, 2]. Magnesium and magnesium based alloys have been deeply investigated because they offer theoretically a high hydrogen capacity (up to 7.6wt.% H in the MgH_2 phase), a low density and a relatively low cost. However, using magnesium hydrides for hydrogen storage applications is hindered by its slow hydrogen absorption and desorption kinetics. The poor hydrogen charge kinetics is usually attributed to surface magnesium oxides and a low diffusion rate of H in MgH_2. Besides, relatively high dehydrogenation temperatures (beyond 600K for MgH_2) are directly linked to the strong Mg-H binding energy [3]. The kinetics and mechanisms of metal hydrides formation has been investigated for quite some time [4] and based on this, several approaches have been proposed to improve the kinetics of hydrogen exchange with Mg: i) the introduction of catalysts or alloying elements to favor the dissociation of H_2 molecules or to reduce the binding energy between Mg and H [5], ii) the introduction of crystalline defects to promote the diffusion of hydrogen [6-11]. However, Mg and Mg alloys oxidize very quickly even at low temperature and at very low O_2 partial pressure. It has been shown for example that at 31°C, under 10^{-5}Pa O_2 a nanoscale layer of MgO form on the surface of a Mg-2.63%Al alloy in few seconds [12]. This is connected to the extremely high affinity of O with Mg giving rise to a very negative formation enthalpy for MgO (about –600 kJ/mol [13]) at room temperature with a corresponding equilibrium O_2 partial pressure below 10^{-35} Pa [14]. This fast oxidation might be a critical issue for the application of Mg or Mg based alloys for solid state hydrogen storage because even under high H_2 pressure some residual O_2 cannot be avoided. Since the formation enthalpy of H_2O is only of -286 kJ/mol [15] and that of MgH_2 of about -75kJ/mol [16], oxidation is unavoidable. Besides, the MgO surface layer reduces the hydrogenation and de-hydrogenation kinetics because it acts as a diffusion barrier against H and it has been reported that after a large number of cycles, the storage_efficiency might decrease [10, 11] which could be attributed to a progressive increase of the volume fraction of MgO. The growth of MgO (fcc structure, Fm-3m space group) is controlled by the diffusion of Mg toward the surface and it is important to note that at a temperature higher than 400°C the kinetics may change due to Mg sublimation [17-19]. Thus, the understanding of the interplay between the oxidation of Mg at low O_2 pressure and the hydride formation (effect of H_2) is of peculiar importance. To this end, the present work investigates the oxidation mechanisms of Mg under low O_2 partial pressure with or without H_2. Since crystalline defects seem to promote hydrogenation, a special emphasis was also given on the role of grain boundaries. Thus, Transmission Electron Microscopy (TEM) observations were carried

out on ultrafine grained Mg under high vacuum conditions (10^{-5} Pa) and under a H_2 pressure of 10^5 Pa at a temperature up to 400°C thanks to an in-situ specimen holder [20, 21].

2. Experimental details

The ultrafine grained Mg material used here was prepared from a commercial purity (99.8%) atomized powder consolidated by severe plastic deformation using High Pressure Torsion [22]. TEM samples were prepared using a Helios (Thermofisher) Plasma Focused Ion Beam (FIB) operated with Xe ions under an accelerating voltage of 30 kV. A tungsten protective layer was deposited on the surface prior to the milling and thinning procedures to limit irradiation damages and implantation of Xe. For in-situ experiments under a pressure of 10^5 Pa of H_2, thin foils were deposited and welded with tungsten on the SiN membrane of the chip used in the in-situ TEM holder. For in-situ experiments without H_2 thin foils were welded on a Cu grid.

TEM observations have been carried out both in conventional mode with a parallel beam (including diffraction) and in scanning mode (STEM) using a Bright Field (BF) and a High Angle Annular Dark Field (HAADF) detector. In-situ TEM experiments under a pressure of 10^5 Pa of H_2 were carried out in a Cs probe corrected JEOL 2100F microscope operated at 200kV. Sample was mounted on an "Atmosphere" Protochips specimen holder, designed as an environmental cell able to withstand high temperature (up to 1000°C) and pressure conditions. A pressure of 10^5 Pa of H_2 was introduced after a complete purge of the system with Ar. The O_2 partial pressure as measured by the spectrometer connected to the specimen holder outlet was 10 Pa during the experiment. A heating rate of 0.3°C s^{-1} was then applied up to 400°C. In-situ TEM observations without H_2 were carried out with a JEOL ARM 200F microscope operated at 200 kV using a double tilt heating holder (Gatan 652 MA) under a pressure of 2 10^{-5}Pa and an O_2 partial pressure below 10^{-5}Pa. The heated volume is much larger with this latter specimen holder which may leads to significant sample drift, gas desorption and possibly to some local temperature overshoot. To minimize these issues, a slightly different heating procedure was applied to reach 400°C. A heating rate of 1°C $s^{-1}$was applied up to 150°C, then 0.5°C s^{-1} up to 300°C where the sample was held during 5min, and then 0.2°C s^{-1} up to 400°C. Thus, the main difference stands at temperatures below 300°C, and it is believed that it does not affect significantly the mechanisms observed at 400°C.

3. Results and discussion

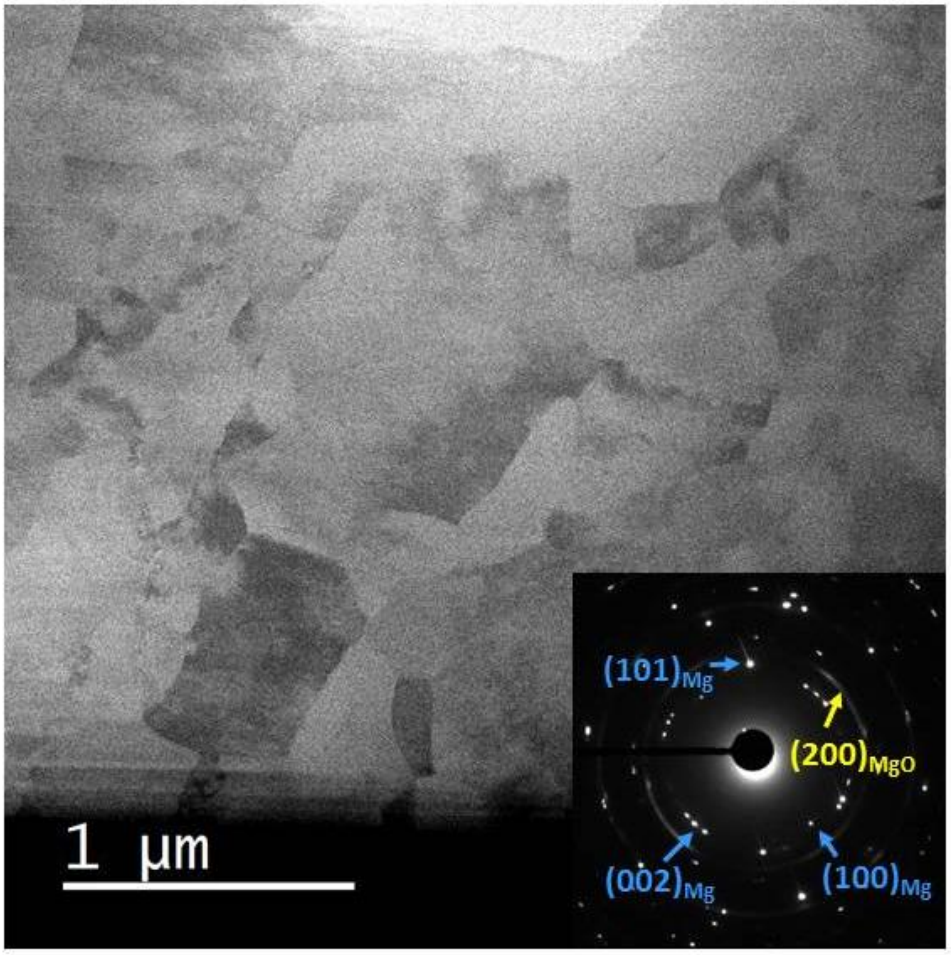

Figure1: *STEM-BF image showing the ultrafine grain structure with large fraction of GBs. Corresponding SAED pattern (aperture size 1.6µm) where spots are indexed with hcp Mg reflections and the diffuse rings are attributed to nanoscaled MgO particles on the foil surface.*

As shown on the STEM Bright Field (BF) image (Fig. 1), the material processed by severe plastic deformation exhibits a submicron grain size, in agreement with an earlier study [22, 23]. The grain size is slightly finer than in bulk Mg processed by SPD [X2] due to a small fraction of nanoscaled oxide particles pinning boundaries. On the selected area electron diffraction (SAED) pattern (Fig. 1 inset), the main spots correspond to hcp Mg and additional diffuse rings to nanoscaled MgO particles. Few of them originate from the initial powder process but most of them have nucleated on the sample surface in the vacuum chamber or during the transfer from the FIB to the TEM.

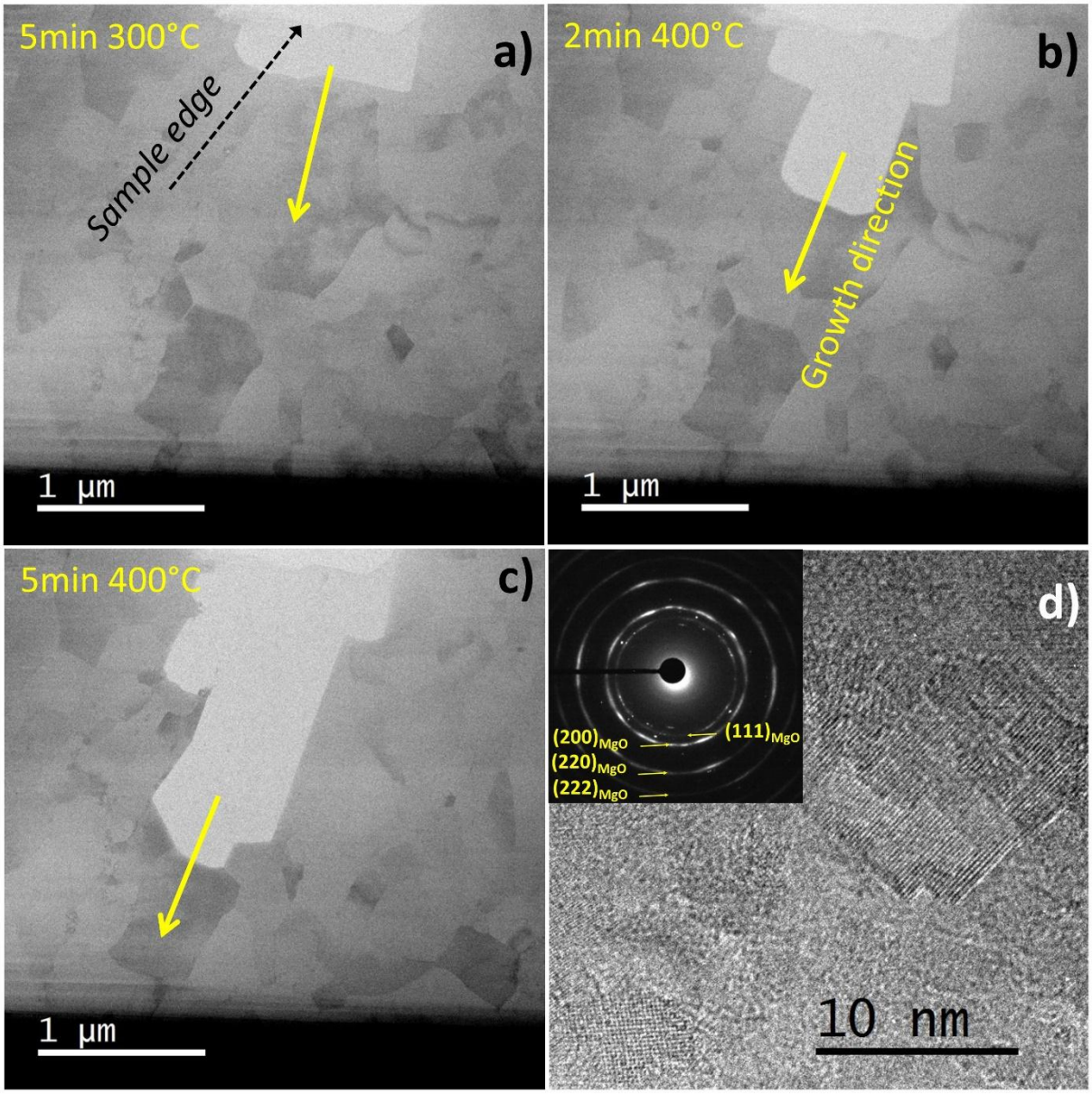

Figure2: *STEM-BF images showing the growth of MgO inside the UFG Mg at low partial pressure of O_2 and H_2 (below 10^{-5} Pa) (a) after 5min at 300°C, (b) after 2min at 400°C and (c) after 5min at 400°C. (d) HRTEM image taken in the oxidized region showing the nanoscaled structure of the MgO oxide, confirmed by the SAED (inset)*

Fig. 2 gathers TEM images obtained during the in-situ heating ramp under vacuum conditions (2 10^{-5} Pa). No significant grain growth occurred and only small local changes of the contrast could be observed. It is the result of recovery of lattice defects that were introduced during the severe plastic deformation processing. This relatively high thermal stability of the UFG structure might be attributed to the pinning of triple lines by the thin foil surface as reported for Al alloys observed by in-situ TEM [24]. Meanwhile, within a very short period of time (5min at 300°C, Fig. 2(a)), a fully transformed area (width 1µm, depth 0.4 µm) with a bright contrast appears at the TEM sample edge

(top of Fig. 2(a)). It quickly grows at 400°C, expanding downward (Fig. 2(b) and 2(c)) along a direction that is perpendicular to the sample edge and reaching a depth of about 2μm. Surprisingly, the lateral growth is more limited and the width remains relatively constant. The high resolution TEM image and the corresponding SAED pattern (Fig. 2(d)) taken in this region show that the original hcp Mg was fully oxidized leading to the formation of nanoscaled MgO particles.

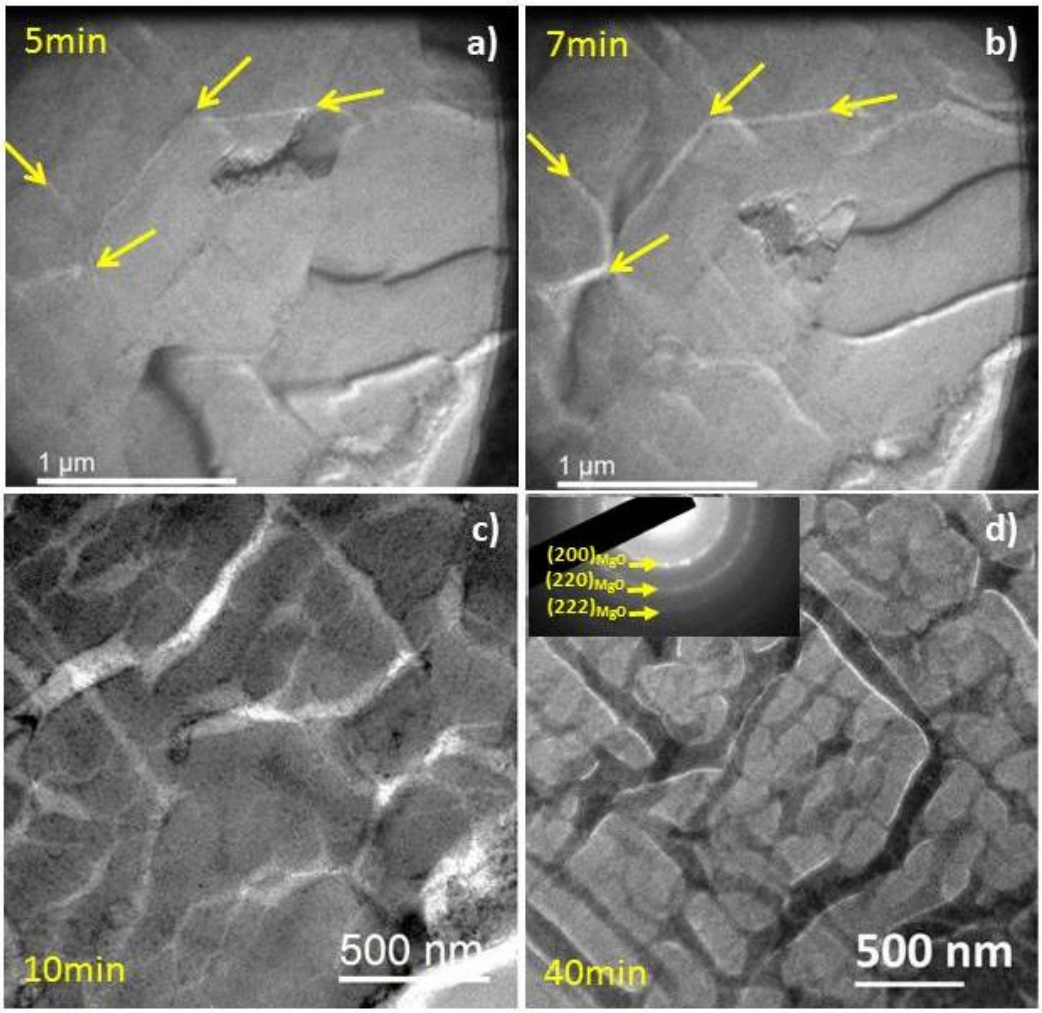

Figure3: *TEM-BF images showing the growth of MgO along GBs (arrowed) in the UFG Mg under 10^5 Pa of H_2 and 10 Pa of O_2, after 5min (a), 7min (b) and 10min (c) at 400°C. STEM-HAADF image after 40min at 400°C and SAED pattern recorded in the oxide (inset) (d)*

Fig. 3 shows a sequence of TEM BF images taken in situ during holding at 400°C under a high partial pressure of H_2 (10^5 Pa). While no significant change was detected below 400°C, at this temperature, the transformation of the structure starts along GBs. Some thin layers with a bright contrast on TEM BF images (arrowed on Fig. 3(a), 3(b)) start to grow after only few minutes at 400°C but no

transformation occurs at the sample edge (located on the bottom right of images). After 10 min the transformation has taken place in the whole microstructure (Fig. 3(c)) and a network covers initial crystalline defects with layers having a thickness ranging from 20 to 100nm. They are darkly imaged on STEM-HAADF images (Fig. 3(d)) and the SAED pattern clearly indicates that they are the result of the nucleation of nanoscaled MgO particles. Although the partial pressure of H_2 was relatively high, it should be noted that MgH_2 phase was not detected during the experiment. For both in-situ TEM experiments (with and without H_2), no significant differences could be seen between regions kept a long time under the electron beam to track real time changes and adjacent regions that have been checked more occasionally. Thus, even if the influence of the electron beam on the transformation cannot be completely ruled out [25], it is believed that it has no major effect and in any case it cannot explain the differences seen under vacuum conditions and under 10^5 Pa H_2.

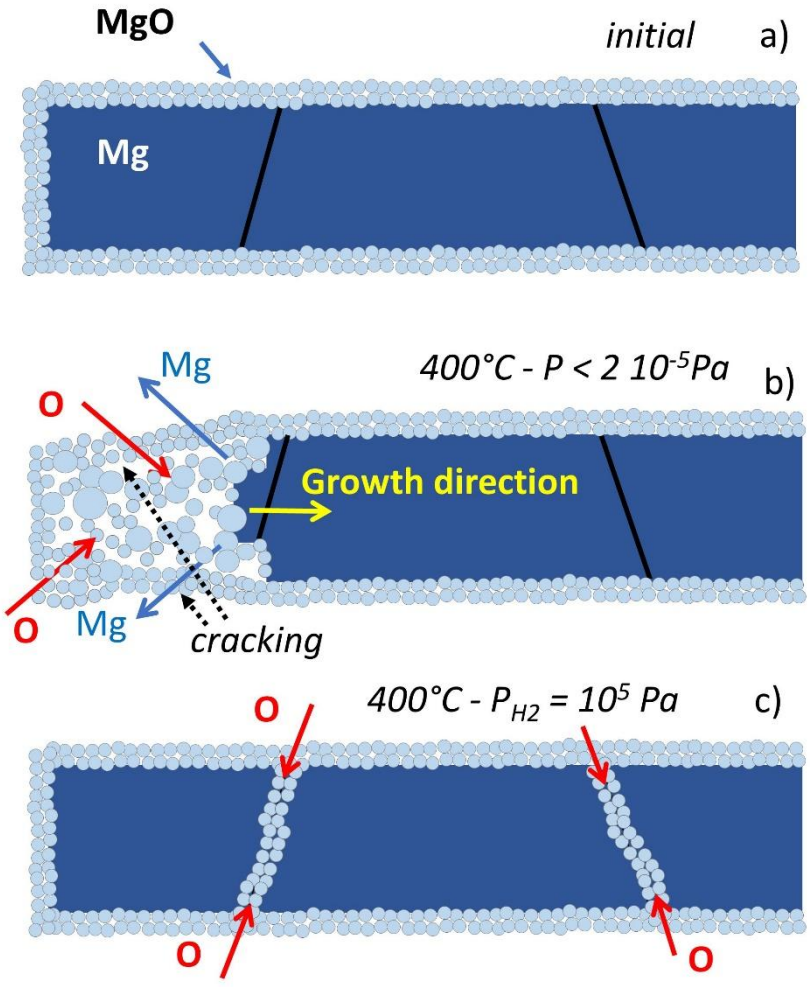

Figure4: *Schematic representation of the evolution of the TEM lamellae during the in-situ experiment. (a) initial state with a thin oxide layer on the surface, (b) oxidation under vacuum conditions, (c) oxidation under a high partial pressure of H_2.*

A comparative schematic representation of the oxidation mechanisms of the UFG Mg under vacuum conditions as well as under 10^5 Pa H_2 is represented in Fig. 4. The initial sample exhibits a nanometer scaled MgO layer on the surface (Fig. 4(a)). It is known that further oxidation of Mg requires the outward diffusion of Mg which is possible only at a temperature higher than room temperature [17-19, 26]. During heating up to 400°C, this layer does not significantly grow because the oxygen partial pressure is low and, thus, the driving force for the outward diffusion of Mg remains rather limited. Besides, the thermal expansion coefficient of Mg being close to that of MgO, the thermal dilatation does not lead to a stress that could break up the layer and promote the oxidation of the underneath Mg. Under vacuum conditions (without H_2) however, it was shown that the oxidized regions could grow along a direction perpendicular to the sample edge (Fig. 2). This region appears with a bright contrast on bright field images, indicating that a significant amount of Mg was sublimated. The extreme situation would be that all Mg contained inside the original MgO crust would evaporate and only a thin layer of MgO would remain such as the hollow structures reported by Pasquini and co-authors [27]. However, in the present situation the intensity of MgO reflections on SAED patterns is much stronger in the reacted region than in the original sample, indicating that some additional MgO nanoparticles have grown. The resulting structure evolution is schematically represented in Fig. 4(b). The reaction is very localized, and it starts at the sample edge. In this location, the curvature is large and it may promote the sublimation of Mg under vacuum conditions [17-19, 26]. Then, local volume changes create stresses leading to cracking of the external MgO crust, facilitating concomitantly the sublimation of Mg and the inward diffusion of O_2. As soon as it starts, this mechanism can promote the nucleation and growth of additional MgO nanoparticles and it would propagate toward a direction perpendicular to the sample edge as observed experimentally. Under 10^5Pa H_2, a much slower kinetic and a more homogenous transformation were observed (Fig. 3). This could be explained by a significantly reduced sublimation of Mg at higher pressure, but it is important to note as well that the atomic mobility of Mg might be also reduced as a result of the interaction between H and vacancies. Then, the high density of crystalline defects and especially GBs resulting from severe plastic deformation play a key role (Fig. 4(c)). They act as fast diffusion paths for O_2 coming from the outside and they are easy nucleation sites for MgO. In principle, this mechanism could also operate under vacuum conditions, but it exhibits such a low kinetic that it does not play a significant role on the overall transformation.

4. Conclusions

We have shown that the oxidation of Mg under low partial pressure of O_2 clearly occurs with different mechanisms under vacuum conditions and under H_2 at atmospheric pressure. Crystalline defects like GBs enhance the hydrogenation of Mg but also promote the nucleation and growth of MgO. This could be detrimental for application of UFG Mg based alloys as solid state storage media for hydrogen. Due to the extremely negative formation enthalpy for MgO, nanoscaled oxide layers are unavoidable on Mg alloys even under high H_2 partial pressure. At low temperature and low O_2 partial pressure, such oxide layers do not grow significantly but during hydrogenation, the growth of hydrides may generate stresses that could break up the oxide layer promoting both the hydride formation (MgH_2, -75 kJ/mol) but also the oxidation (MgO, -600kJ/mol). This feature is another important reason to develop Mg alloys with dehydrogenation temperature as low as possible.

Acknowledgements

Some of the TEM experiments have been carried out on the GENESIS facility which is supported by the Région Normandie, the Métropole Rouen Normandie, the CNRS via LABEX EMC3 and the French National Research Agency as a part of the program “Investissements d’avenir” with the reference ANR-11-EQPX-0020. Part of this work was also supported by the French State via the program "Investment in the future" operated by the National Research Agency (ANR) and referenced by ANR-11-LABX-0008-01 (Labex DAMAS).

References

[1] Kenneth E. Cox and K.D. Williamson, Hydrogen: its technology and implications, vol. 2, CRC Press (2018), Taylor and Francis, Bocca Raton, FL, USA

[2] L. Schlapbach, A. Züttel, Nature 414 (2001) 353-358.

[3] I.P. Jain, C. Lal, A. Jain, Int. J. Hydrogen Energy 35 (2010) 5133-5144.

[4] Joseph Bloch, Moshe H. Mintz, Journal of Alloys and Compounds 253-254 (1997) 529-541

[5] Kaveh Edalati, Ryoko Uehiro, Yuji Ikeda, Hai-Wen Li, Hoda Emami, Yaroslav Filinchuk, Makoto Arita, Xavier Sauvage, Isao Tanaka, Etsuo Akiba and Zenji Horita, Acta Materialia 149 (2018) 88-96

[6] Toshifumi Hongo, Kaveh Edalati, Makoto Arita, Junko Matsuda, Etsuo Akiba and Zenji Horita, Acta Mater 92 (2015) 46-54

[7] Stephen D. House, John J. Vajo, Chai Ren, Angus A. Rockett, Ian M. Robertson, Acta Mater

86 (2015) 55-68

[8] D.R. Leiva, A.M. Jorge, T.T. Ishikawa and W.J. Botta, Materials Transactions, Vol 60 (2019) 1561 - 1570.

[9] K. Edalati, A. Yamamoto, Z. Horita, T. Ishihara, Scripta Mater 64 (2011) 880 - 883.

[10] M. Krystiana, M.J. Zehetbauer, H. Kropik,1, B. Mingler, G. Krexner, Journal of Alloys and Compounds 509S (2011) S449–S455

[11] Andreas Grill, Jelena Horky, Ajit Panigrahi, Gerhard Krexner, Michael Zehetbauer, Int. jour. of hydrogen energy 40 (2015) 17144-17152

[12] L.P.H. Jeurgens, M.S. Vinodh, E.J. Mittemeijer, Mater 56 (2008) 4621-4634

[13] H.A. Wriedt, The Mg-O (Magnesium-Oxygen) System, Bulletin of Alloy Phase Diagrams Vol. 8 No. 3 (1987) 227-233

[14] Masakatsu Hasegawa, Treatise on Process Metallurgy, Chapter 3.3 - Ellingham Diagram, Editor(s): Seshadri Seetharaman, Elsevier, 2014, Pages 507-516

[15] J.D. Cox, D.D. Wagman, V.A. Medvedev, CODATA Key Values for Thermodynamics, Hemisphere Publishing Corp., New York, 1984

[16] J. F. Stampfer, C. E. Holley and J. F. Suttle, J. Am. Chem. Soc. 82, 14 (1960) 3504-3508.

[17] Qiyang Tan, Andrej Atrens, Ning Mo, Ming-Xing Zhang, Corrosion Science 112 (2016) 734-759

[18] F. Czerwinski, Acta Materialia 50 (2002) 2639–2654

[19] V. Fournier, P. Marcus and I. Olefjord, Surf. Interface Anal. 34 (2002) 494–497

[20] Tadahiro Yokosawa, Tuncay Ala, Gregory Pandraud, Bernard Dam, Henny Zandbergen, Ultramicroscopy 112 (2012) 47-52

[21] G. Melinte, S. Moldovan, C. Hirlimann, W.Baaziz, S. Begin-Colin, C. Pham-Huu, and O. Ersen, ACS CATALYSIS 7 (2017) 5941-5949

[22] Subrata Panda, Jean-Jacques Fundenberger, Yajun Zhao, Jianxin Zou, Laszlo S. Toth, Thierry Grosdidier, International Journal of Hydrogen Energy 42 (2017) 22438-22448.

[23] Subrata Panda, Jean-Jacques, Laszlo S. Toth, Jianxin Zou, Thierry Grosdidier, Materials, 11 (2018) 1335.

[24] E.V. Bobruk, X. Sauvage, A.M. Zakirov and N.A. Enikeev, Rev. Adv. Mater. Sci. 55 (2018) 61-68.

[25] Huai-Ruo Zhang, Ray Egerton, Marek Malac, Nuclear Instruments and Methods in Physics Research Section B: Beam Interactions with Materials and Atoms 316 (2013) 137-143Zijao

[26] Zhang, Xiaoquian Fu, Minmin Mao, Qian Yu, Scott X. Mao, Jixue Li, Ze Zhang, Nano Research 9 (2016) 2796-2802

[27] Luca Pasquini, Amelia Montone, Elsa Callini, Marco Vittori Antisari, and Ennio Bonetti, Applied Physics Letters 99 (2011) 021911